Updated measurement of the $e^+e^- \to \omega\pi^0 \to \pi^0\pi^0\gamma$ cross section with the SND detector

M. N. Achasov,[1,2] A. Yu. Barnyakov,[1,2] K. I. Beloborodov,[1,2] A. V. Berdyugin,[1,2] D. E. Berkaev,[1,2] A. G. Bogdanchikov,[1] A. A. Botov,[1] T. V. Dimova,[1,2] V. P. Druzhinin,[1,2] V. B. Golubev,[1,2] L. V. Kardapoltsev,[1,2,*] A. S. Kasaev,[1] A. G. Kharlamov,[1,2] A. N. Kirpotin,[1] D. P. Kovrizhin,[1,2] I. A. Koop,[1,2,3] A. A. Korol,[1,2] S. V. Koshuba,[1] K. A. Martin,[1] A. E. Obrazovsky,[1] E. V. Pakhtusova,[1] Yu. A. Rogovsky,[1,2] A. I. Senchenko,[1] S. I. Serednyakov,[1,2] Z. K. Silagadze,[1,2] Yu. M. Shatunov,[1,2] D. A. Shtol,[1,2] D. B. Shwartz,[1,2] A. N. Skrinsky,[1] I. K. Surin,[1,2] and A. V. Vasiljev[1,2]

[1]*Budker Institute of Nuclear Physics, SB RAS, Novosibirsk 630090, Russia*
[2]*Novosibirsk State University, Novosibirsk 630090, Russia*
[3]*Novosibirsk State Technical University, Novosibirsk 630092, Russia*

(Received 7 October 2016; published 1 December 2016)

We analyze a 37 pb^{-1} data sample collected with the SND detector at the VEPP-2000 e^+e^- collider in the center-of-mass energy range 1.05–2.00 GeV and present an updated measurement of the $e^+e^- \to \omega\pi^0 \to \pi^0\pi^0\gamma$ cross section. In particular, we correct the mistake in radiative correction calculation made in our previous measurement based on a part of the data. The measured cross section is fitted with the vector meson dominance model with three ρ-like states and used to test the conserved vector current hypothesis in the $\tau^- \to \omega\pi^-\nu_\tau$ decay.

DOI: 10.1103/PhysRevD.94.112001

I. INTRODUCTION

The process $e^+e^- \to \omega\pi^0$ is one of the dominant processes contributing to the total hadronic cross section at the center-of-mass (c.m.) energy between 1 and 2 GeV. The measurement of the $e^+e^- \to \omega\pi^0$ cross section provides information about properties of excited ρ-like states and can be used to check the relation between the cross section and the spectral function in the $\tau \to \omega\pi^-\nu_\tau$ decay following from the conserved vector current hypothesis [1].

The $e^+e^- \to \omega\pi^0$ cross section was measured in the ND [2], SND [3–5], and CMD-2 [6,7] experiments at the VEPP-2M collider at c.m. energies below 1.4 GeV, in the KLOE experiment [8] in the ϕ-meson region, and in the DM2 experiment [9] in the 1.35–2.4 GeV energy range.

In the SND experiment [10–13] at the VEPP-2000 e^+e- collider [14] the $e^+e^- \to \omega\pi^0$ cross section is studied in the five-photon final state when the ω-meson decays to $\pi^0\gamma$. The result of the study based on data collected in 2010 and 2011 was published in Ref. [15]. However, a mistake was made in the calculation of the radiative corrections in Ref. [15], which led to incorrect measurement of the Born $e^+e^- \to \omega\pi^0$ cross section.

In this paper we reanalyze the 2010–2011 data sample (25 pb^{-1}) and add data collected in 2012 (12 pb^{-1}). The analysis is very close to that described in Ref. [15]. We correct the mistake in the radiative correction calculation and slightly modify the selection criteria of $e^+e^- \to \gamma\gamma$ events for luminosity measurement. The analysis uses an updated version of the event reconstruction and simulation software. Therefore, the values of the efficiency corrections and systematic uncertainties are changed compared with those in Ref. [15].

In this analysis we use the corrected values of the c.m. energy (E) obtained in Ref. [16]. The accuracy of the energy measurement is 6 MeV and 2 MeV for 2011 and 2012 experiments, respectively. The 2010 and 2011 data are combined assuming that the energy calibration is the same for the 2010 and 2011 experiments.

II. LUMINOSITY MEASUREMENT

Following the previous work [15], we use the $e^+e^- \to \gamma\gamma$ process for the luminosity measurement. Similar to the process under study, it does not contain charged particles in the final state. Therefore, some uncertainties on the cross section measurement cancel as a result of the luminosity normalization.

We select events with at least two photons and no charged particles. The number of hits in the detector drift chamber is required to not exceed 5. The energies of two most energetic photons in an event must be larger than $0.3E$. The azimuthal ($\phi_{1,2}$) and polar ($\theta_{1,2}$) angles of these photons must satisfy the following conditions: $\|\phi_1-\phi_2|-180°| < 11.5°$, $|\theta_1+\theta_2-180°| < 17.2°$, and $(180°-|\theta_1-\theta_2|)/2 > 54°$.

The integrated luminosity measured for each energy point is listed in Table I. The systematic uncertainty on the luminosity measurement estimated to be 1.4%.

III. EVENT SELECTION

For the process under study $e^+e^- \to \omega\pi^0 \to \pi^0\pi^0\gamma \to 5\gamma$, candidate events must have at least five photons and no charged particles. The number of hits in the drift chamber is required to not exceed 5. The normalized total energy

*l.v.kardapoltsev@inp.nsk.su

TABLE I. The c.m. energy (E), integrated luminosity (L), detection efficiency (ε), number of selected signal events (N_s), radiative-correction factor ($1+\delta$), and measured Born cross section (σ). The quoted errors on N_s and σ are statistical. The systematic uncertainty on the cross section is 2.7% at $E < 1.59$ GeV, 3.5% at $1.59 < E < 1.79$ GeV, and 5.2% in energy range $E > 1.79$ GeV.

E (MeV)	L (nb^{-1})	ε (%)	N_s	$1+\delta$	σ (nb)
1047 ± 6	352	35.1	105 ± 13	0.895	0.95 ± 0.11
1075 ± 6	542	35.3	180 ± 17	0.903	1.04 ± 0.09
1097 ± 6	839	35.5	290 ± 19	0.905	1.08 ± 0.07
1124 ± 6	520	35.9	213 ± 17	0.907	1.26 ± 0.11
1151 ± 6	412	36.3	178 ± 13	0.912	1.3 ± 0.1
1174 ± 6	536	36.3	230 ± 21	0.913	1.29 ± 0.12
1196 ± 6	1063	36.0	485 ± 25	0.913	1.39 ± 0.07
1223 ± 6	554	37.2	251 ± 19	0.913	1.33 ± 0.11
1245 ± 6	432	37.3	184 ± 14	0.913	1.25 ± 0.12
1273 ± 6	495	37.1	257 ± 21	0.914	1.53 ± 0.13
1277 ± 2	677	37.3	320 ± 21	0.917	1.38 ± 0.09
1295 ± 6	1266	37.5	678 ± 31	0.915	1.56 ± 0.07
1323 ± 6	526	38.2	282 ± 23	0.915	1.54 ± 0.12
1344 ± 6	553	37.8	289 ± 24	0.917	1.5 ± 0.13
1357 ± 2	756	37.8	418 ± 29	0.915	1.6 ± 0.11
1374 ± 6	572	37.5	304 ± 23	0.916	1.55 ± 0.12
1394 ± 6	1042	37.3	574 ± 32	0.921	1.61 ± 0.09
1423 ± 6	598	37.9	372 ± 22	0.922	1.78 ± 0.1
1435 ± 2	917	37.4	528 ± 27	0.923	1.67 ± 0.09
1443 ± 6	428	37.4	218 ± 17	0.926	1.47 ± 0.12
1471 ± 6	596	37.6	285 ± 20	0.931	1.37 ± 0.1
1494 ± 6	1954	38.1	990 ± 40	0.938	1.42 ± 0.06
1515 ± 2	829	37.6	355 ± 22	0.944	1.21 ± 0.08
1522 ± 6	478	37.6	251 ± 17	0.945	1.48 ± 0.1
1543 ± 6	546	38.2	225 ± 16	0.952	1.13 ± 0.08
1572 ± 6	510	37.4	170 ± 15	0.965	0.93 ± 0.08
1595 ± 2	903	37.3	264 ± 19	0.976	0.77 ± 0.07
1594 ± 6	820	36.7	226 ± 19	0.974	0.8 ± 0.06
1623 ± 6	508	37.6	132 ± 14	0.992	0.7 ± 0.08
1643 ± 6	471	36.4	94 ± 11	1.006	0.54 ± 0.07
1669 ± 6	454	36.2	75 ± 11	1.021	0.45 ± 0.07
1674 ± 2	837	35.7	127 ± 13	1.025	0.41 ± 0.04
1693 ± 6	827	35.1	105 ± 13	1.043	0.35 ± 0.04
1716 ± 2	455	34.6	50 ± 7	1.059	0.3 ± 0.05
1723 ± 6	507	35.5	32 ± 7	1.060	0.17 ± 0.04
1742 ± 6	509	34.4	32 ± 8	1.077	0.17 ± 0.04
1758 ± 2	797	33.8	50 ± 10	1.081	0.17 ± 0.04
1774 ± 6	530	34.1	38 ± 7	1.072	0.2 ± 0.04
1798 ± 2	919	32.2	59 ± 10	1.066	0.14 ± 0.03
1793 ± 6	752	32.8	38 ± 7	1.058	0.19 ± 0.03
1826 ± 6	488	33.4	16 ± 5	1.037	0.09 ± 0.03
1840 ± 2	953	31.9	38 ± 8	1.024	0.12 ± 0.03
1849 ± 6	403	31.7	9 ± 5	1.020	0.07 ± 0.04
1871 ± 6	641	31.6	20 ± 6	1.002	0.1 ± 0.03
1874 ± 2	835	30.7	32 ± 6	1.004	0.12 ± 0.02
1893 ± 6	579	31.4	24 ± 6	0.993	0.13 ± 0.03
1903 ± 2	867	29.9	16 ± 5	0.989	0.08 ± 0.03
1901 ± 6	559	29.6	13 ± 5	0.986	0.06 ± 0.02
1926 ± 2	614	29.6	14 ± 5	0.978	0.08 ± 0.03
1927 ± 6	562	29.4	16 ± 4	0.979	0.1 ± 0.03
1945 ± 2	823	28.8	15 ± 5	0.973	0.06 ± 0.02
1953 ± 6	402	29.3	4 ± 3	0.970	0.03 ± 0.03
1967 ± 2	679	27.7	12 ± 4	0.970	0.06 ± 0.03
1978 ± 6	467	27.1	$5.6^{+6.5}_{-3.0}$	0.970	$0.05^{+0.05}_{-0.02}$
1989 ± 2	578	27.6	10 ± 3	0.964	0.06 ± 0.02
2005 ± 6	546	27.2	10 ± 4	0.965	0.07 ± 0.03

deposition in the calorimeter $E_{\rm tot}/E > 0.5$. For events passing this selection, kinematic fits to the $e^+e^- \to 5\gamma$ and $e^+e^- \to \pi^0\pi^0\gamma$ hypotheses are performed. The goodness of the fits is characterized by the χ^2 parameters, $\chi^2_{5\gamma}$ and $\chi^2_{\pi^0\pi^0\gamma}$. For events with more than five photons, all five-photon combinations are tested and the one with minimal $\chi^2_{\pi^0\pi^0\gamma}$ is used. The following cuts on parameters obtained after the kinematic fits are applied:

(i) $\chi^2_{5\gamma} < 30$

(ii) $\chi^2_{\pi^0\pi^0\gamma} - \chi^2_{5\gamma} < 10$,

(iii) at least one of the two $\pi^0\gamma$ invariant masses satisfies the condition $|m_{\pi^0\gamma} - M_\omega| < 200$ MeV/c^2, where M_ω is the ω-meson nominal mass [17].

The number of signal events is determined from the fit to the $\pi^0\gamma$ mass spectrum with a sum of signal and background distributions. The fitting procedure is described in detail in Ref. [15]. The result of the fit to the data spectrum for the energy point $E = 1494$ MeV (two entries per event) is shown in Fig. 1. The ω-meson peak is clearly seen in the spectrum. The dashed curve represents the background

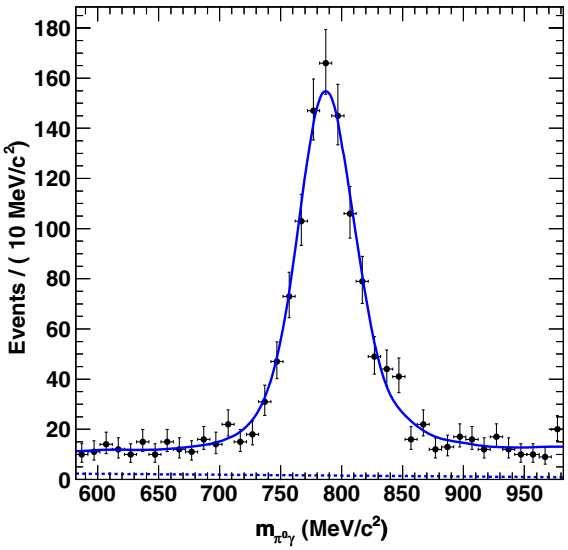

FIG. 1. The distribution of the $\pi^0\gamma$-invariant mass for selected data events (points with error bars) with $E = 1494$ MeV. The curve is the result of the fit by the sum of the signal and background distribution. The dashed curve represents the background contribution.

contribution. The fitted number of signal events for each energy point is listed in Table I.

IV. THE $e^+e^- \to \omega\pi^0 \to \pi^0\pi^0\gamma$ BORN CROSS SECTION

The experimental values of the Born cross section is determined as

$$\sigma(E_i) = \frac{N_{s,i}}{L_i \varepsilon_i (1+\delta(E_i))}, \quad (1)$$

where $N_{s,i}$, L_i, ε_i, and $\delta(E_i)$ are the number of selected signal events, integrated luminosity, detection efficiency, and radiative correction for the ith energy point.

The detection efficiency for the process under study is determined using Monte Carlo (MC) simulation and then corrected by $(-3.9 \pm 0.7)\%$ to take into account data-MC simulation difference in the detector response. The largest contribution to the correction comes from the data-MC simulation differences in the $\chi^2_{5\gamma}$ and $\chi^2_{\pi^0\pi^0\gamma} - \chi^2_{5\gamma}$ distributions. It is estimated by changing the limits of the conditions on $\chi^2_{5\gamma}$ and $\chi^2_{\pi^0\pi^0\gamma} - \chi^2_{5\gamma}$ from 30 to 50 and from 10 to 50, respectively, and found to be $(-3.9 \pm 0.5)\%$. The photon conversion probability before the drift chamber is measured using $e^+e^- \to \gamma\gamma$ events. The correction due the data-MC simulation difference in photon conversion is -0.8% with a negligible uncertainty. The presence of beam-generated spurious photons also changes the detection efficiency. To estimate this effect we use beam-background events recorded during experiment with a special random trigger and merge them with simulated events. The obtained efficiency correction varies from 0.3% to 1.3% depending on experimental conditions. We use the average value of this correction $(0.8 \pm 0.5)\%$.

The found detection efficiency ε_r is a function of two parameters: the c.m. energy E and the energy of the extra photon E_r emitted from the initial state. The efficiency in Eq. (1) $\varepsilon_i = \varepsilon_r(E_i, E_r = 0)$.

The radiative correction is determined from the fit to the visible cross-section data $[\sigma_{\rm vis}(E_i) = N_{s,i}/L_i]$ with the function

$$\sigma_{\rm vis}(E) = \sigma(E)\varepsilon(E)(1+\delta(E) = \int_0^{x_{\rm max}} \varepsilon_r(E, xE/2) F(x,E) \sigma(E\sqrt{1-x}) dx, \quad (2)$$

where $F(x,E)$ is a function describing the probability to emit extra photons with the total energy $xE/2$ from the initial state [18]. The Born cross section is described by the following formula [15]:

$$\sigma(E) = \frac{4\pi\alpha^2}{3E^3} |F_{\omega\pi\gamma}(E^2)|^2 P_f(E) B(\omega \to \pi^0\gamma), \quad (3)$$

where α is the fine-structure constant, $F_{\omega\pi\gamma}(E^2)$ is the $\gamma^* \to \omega\pi^0$ transition form factor, $B(\omega \to \pi^0\gamma)$ is the branching fraction for the $\omega \to \pi^0\gamma$ decay, and $P_f(E)$ is the phase-space factor. In the narrow ω-resonance approximation $P_f(E) = q_\omega^3$, where q_ω is the ω-meson momentum. The transition form factor is parametrized in the vector meson dominance (VMD) model as a sum of the $\rho(770)$, $\rho(1450)$, and $\rho(1700)$ resonance contributions,

$$F_{\omega\pi\gamma}(E^2) = \frac{g_{\rho\omega\pi}}{f_\rho}\left(\frac{m_\rho^2}{D_\rho} + A_1 e^{i\varphi_1}\frac{m^2_{\rho(1450)}}{D_{\rho(1450)}} + A_2 e^{i\varphi_2}\frac{m^2_{\rho(1700)}}{D_{\rho(1700)}}\right), \quad (4)$$

where $g_{\rho\omega\pi}$ is the $\rho \to \omega\pi$ coupling constant, f_ρ is the $\gamma^* \to \rho$ coupling constant calculated from the $\rho \to e^+e^-$ decay width, $D_{\rho_i}(E) = m^2_{\rho_i} - E^2 - \imath E\Gamma_{\rho_i}(E)$, and m_{ρ_i} and $\Gamma_{\rho_i}(E)$ are the mass and width of the resonance ρ_i. The formula for $\Gamma_{\rho(770)}(E)$ is given in Ref. [15]. For the $\rho(1450)$ and $\rho(1700)$ resonances, the energy-independent widths are used.

The free fit parameters are $g_{\rho\omega\pi}$, $m_{\rho(1450)}$, $\Gamma_{\rho(1450)}$, and the relative amplitudes (A_i) and phases (φ_i) for the $\rho(1450)$ and $\rho(1700)$ resonances. Because the $\rho(1700)$ contribution is found to be small, its mass and width are fixed at their Particle Data Group (PDG) values [17]. The data from this work are fitted together with the cross-section data obtained in the SND@VEPP-2M [3,4] and KLOE [8] experiments. The model describes data well ($\chi^2/\nu = 71/73$, where ν is the number of degrees of freedom). The obtained fit parameters listed in Table II (Model 1) are used to calculate the radiative corrections.

TABLE II. The fitted parameters of the $e^+e^- \to \omega\pi^0$ cross-section model.

lccc Parameter	Model 1	Model 2	Model 3
$g_{\rho\omega\pi}$, GeV^{-1}	15.9 ± 0.4	16.5 ± 0.2	⋯
A_1	0.175 ± 0.016	0.137 ± 0.006	0.251 ± 0.006
A_2	0.014 ± 0.004	$\equiv 0$	0.027 ± 0.003
$M_{\rho(1450)}$, MeV	1510 ± 7	1499 ± 4	1516 ± 10
$\Gamma_{\rho(1450)}$, MeV	440 ± 40	367 ± 13	500 ± 30
$M_{\rho(1700)}$, MeV	$\equiv 1720$	⋯	$\equiv 1720$
$\Gamma_{\rho(1700)}$, MeV	$\equiv 250$	⋯	$\equiv 250$
φ_1, deg.	124 ± 17	122 ± 8	162 ± 6
φ_2, deg.	-63 ± 21	⋯	-24 ± 10
χ^2/ν	71/73	85/75	83/74

The experimental values of the Born cross section obtained using Eq. (1) are listed in Table I together with the values of the detection efficiency and radiative correction. The quoted errors are statistical. The systematic uncertainties (see Ref. [15] for details) are summarized in Table III for three energy intervals.

V. DISCUSSION

The measured $e^+e^- \to \omega\pi^0 \to \pi^0\pi^0\gamma$ Born cross section is shown in Fig. 2 in comparison with the previous

TABLE III. The systematic uncertainties (%) on the measured cross section for different energy regions. The total uncertainty is the sum of all the contributions in quadrature.

Source	$E < 1.59$ GeV	$1.59 < E < 1.79$ GeV	$E > 1.79$ GeV
Luminosity	1.4	1.4	1.4
Selection criteria	0.5	0.5	0.5
Beam background	0.5	0.5	0.5
Radiative correction	1	1	3
Interference with $\rho^0\pi^0$	2	3	4
Total	2.7	3.5	5.2

measurements [3,4,7,9]. Our data are in agreement with the SND@VEPP-2M and CMD-2 measurements below 1.4 GeV, but exceed the DM2 data in the energy region 1.35–1.75 GeV. After correction of the mistake made in Ref. [15], the Born cross section increases by 2% at $E = 1.1$ GeV, 6% at 1.4 GeV, and 12% at 1.6 GeV. Dramatic changes are observed above 1.8 GeV, where the cross section in Ref. [15] was consistent with zero. Compared with Ref. [15], the systematic uncertainty is improved from 3.4% to 2.7% below 1.6 GeV, mainly due to decrease of the uncertainties associated with luminosity measurement and photon conversion. The new calculation of the radiation correction leads to a significant reduction (from 100% to 5.2%) of the systematic uncertainty above 1.8 GeV.

The measured cross section is well described by the VDM model with two excited ρ-like resonances. The fitted mass and width of the $\rho(1450)$ resonance listed in Table II are in reasonable agreement with the corresponding PDG values. The contribution of the $\rho(1700)$ resonance is small. We also perform a fit with one excited resonance (Model 2 in Table II). From the difference of the χ^2 values for Models 1 and 2 we determine that the significance of the $\rho(1700)$ contribution is 3.7σ.

Using the fit results and the branching fraction $B(\omega \to \pi^0\gamma) = (8.88 \pm 0.18)\%$ measured by SND [19], the products of the branching fractions are calculated to be

$$B(\rho(1450) \to e^+e^-)B(\rho(1450) \to \omega\pi^0) = (2.1 \pm 0.4) \times 10^{-6}, \quad (5)$$

$$B(\rho(1700) \to e^+e^-)B(\rho(1700) \to \omega\pi^0) = (0.09 \pm 0.05) \times 10^{-6}. \quad (6)$$

In Fig. 3 we show our result on the normalized $\gamma^* \to \omega\pi^0$ transition form factor in comparison with the data obtained from the $\omega \to \pi^0\mu^+\mu^-$ decay in the NA60 experiment [20]. The $F_{\omega\pi\gamma}(0)$ value is calculated from the $\omega \to \pi\gamma$ decay width measured by SND [3] using the formula

$$|F_{\omega\pi\gamma}(0)|^2 = \frac{3\Gamma(\omega \to \pi^0\gamma)}{\alpha P_\gamma^3}, \quad (7)$$

where P_γ is the decay photon momentum.

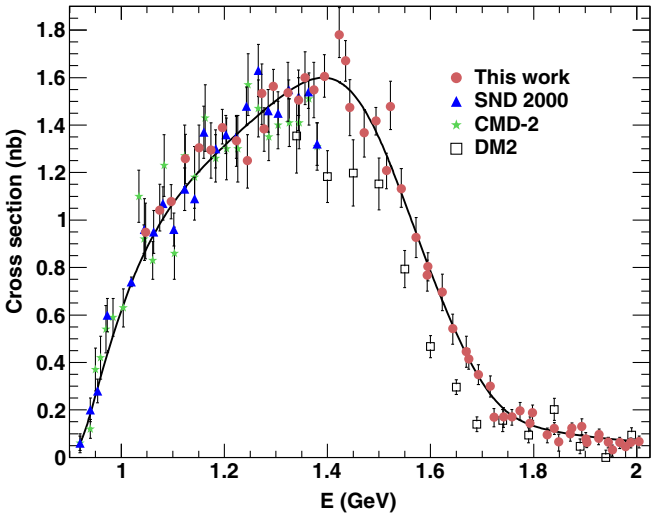

FIG. 2. The cross section for $e^+e^- \to \omega\pi^0 \to \pi^0\pi^0\gamma$ measured in this work (circles), and in the SND@VEPP-2M [3,4] (triangles), CMD-2 [7] (stars), and DM2 [9] (squares) experiments. Only statistical errors are shown. The curve is the result of the fit to SND 2000 and SND 2013 data described in the text (Model 1).

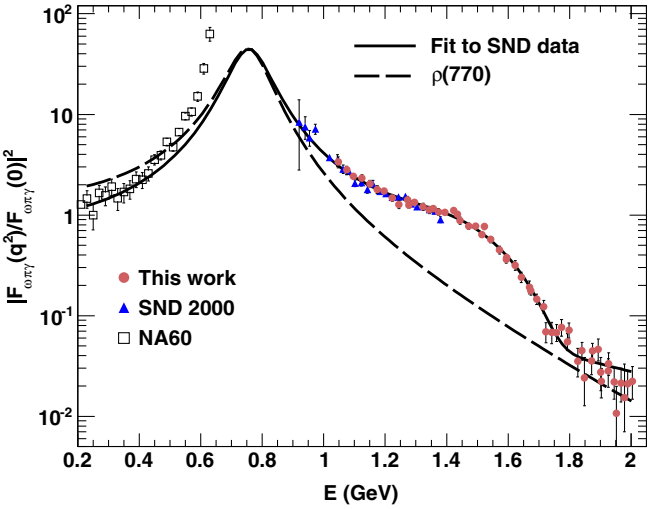

FIG. 3. The $\gamma^* \to \omega\pi^0$ transition form factor. The points with error bars represent data from this work (circles), Ref. [3] (triangles), and Ref. [20] (squares). Only statistical errors are shown. The curve is the result of of the fit to the $e^+e^- \to \omega\pi^0$ cross-section data. The dashed curve shows the $\rho(770)$ contribution.

The form-factor model given by Eq. (4) with parameters from Table II for Model 1 and 2 describes well $e^+e^- \to \omega\pi^0$ data, but does not provide form-factor normalization at zero, and, therefore, cannot be used at low E^2 corresponding to data from ω decays. We modify our form-factor model to provide correct normalization at zero,

$$F_{\omega\pi\gamma}(E^2) = F_{\omega\pi\gamma}(0)\left(\frac{m_\rho^2}{D_\rho} + A_1 e^{i\varphi_1}\frac{m^2_{\rho(1450)}}{D_{\rho(1450)}} + A_2 e^{i\varphi_2}\frac{m^2_{\rho(1700)}}{D_{\rho(1700)}}\right)/(1 + A_1 e^{i\varphi_1} + A_2 e^{i\varphi_2}). \quad (8)$$

The parameters of this model obtained from the fit to the SND and KLOE data are listed in Table II (Model 3). The normalization requirement leads to worse but still acceptable fit quality. The fitted curve is shown in Fig. 3. It is seen that the VMD model cannot describe simultaneously the $e^+e^- \to \omega\pi^0$ and $\omega \to \pi^0\mu^+\mu^-$ data.

The conserved vector current (CVC) hypothesis and isospin symmetry give the relation between the $e^+e^- \to \omega\pi^0$ cross section and the $\tau^- \to \omega\pi^-\nu_\tau$ decay width [1,21]

$$\Gamma(\tau^- \to \omega\pi^-\nu_\tau) = \frac{G_F^2|V_{ud}|^2}{64\pi^4\alpha^2 m_\tau^3}\int^{m_\tau} q^3(m_\tau^2 - q^2)^2(m_\tau^2 + 2q^2)\sigma_{\omega\pi^0}(q)dq, \quad (9)$$

where $|V_{ud}|$ is the Cabibbo-Kobayashi-Maskawa matrix element, m_τ is the τ lepton mass, and G_F is the Fermi constant. Integrating the fitted curve shown in Fig. 2 we obtain $\Gamma(\tau^- \to \omega\pi^-\nu_\tau)B(\omega \to \pi^0\gamma) = (3.76 \pm 0.04 \pm 0.10) \times 10^{-6}$ eV. Using the PDG value of the τ lifetime [17] and the SND result for $B(\omega \to \pi^0\gamma)$ [19] we calculate

$$B(\tau^- \to \omega\pi^-\nu_\tau) = (1.87 \pm 0.02 \pm 0.07) \times 10^{-2}. \quad (10)$$

The calculated branching fraction is in good agreement with the experimental value $(1.96 \pm 0.08) \times 10^{-2}$ that was obtained as a difference of the PDG [17] values for $B(\tau^- \to \omega h^-\nu_\tau)$ and $B(\tau^- \to \omega K^-\nu_\tau)$.

VI. SUMMARY

The $e^+e^- \to \omega\pi^0 \to \pi^0\pi^0\gamma$ cross section has been measured in the energy range of 1.05–2.00 GeV in the experiment with the SND detector at the VEPP-2000 e^+e^- collider. We correct the mistake in the radiative correction calculation made in our previous work [15] and increase the statistics. The results presented in this paper correct and supersede the results of Ref. [15].

Our data on the $e^+e^- \to \omega\pi^0$ cross section in the energy range 1.4–2.0 GeV are most accurate to date. Below 1.4 GeV they agree with the SND@VEPP-2M [3] and CMD-2 [7] measurements. Significant disagreement is observed with DM2 data [9] in the energy range 1.35–1.75 GeV.

Data on the $e^+e^- \to \omega\pi^0$ cross section are well fitted by the VMD model with the $\rho(770)$, $\rho(1450)$, and $\rho(1700)$ resonances. However, this model cannot describe simultaneously the data on the $\gamma^* \to \omega\pi^0$ transition form obtained from the $\omega \to \pi^0\mu^+\mu^-$ decay [20].

We have also tested the CVC hypothesis calculating the branching fraction for the $\tau^- \to \omega\pi^-\nu_\tau$ decay from our $e^+e^- \to \omega\pi$ data. The calculated branching fraction agrees with the measured value within the experimental uncertainty of about 5%.

ACKNOWLEDGMENTS

This work is partly supported by the Russian Foundation for Basic Research Grant No. 15-02-01037. Part of this work related to the photon reconstruction algorithm in the electromagnetic calorimeter is supported by the Russian Science Foundation (Project No. 14-50-00080).

[1] Y.-S. Tsai, Phys. Rev. D **4**, 2821 (1971); **13**, 771(E) (1976).
[2] S. I. Dolinsky *et al.* (ND Collaboration), Phys. Lett. B **174**, 453 (1986).
[3] M. N. Achasov *et al.* (SND Collaboration), Phys. Lett. B **486**, 29 (2000).
[4] V. M. Aulchenko *et al.* (SND Collaboration), Zh. Eksp. Teor. Fiz. **117**, 1067 (2000) [J. Exp. Theor. Phys. **90**, 927 (2000)].
[5] M. N. Achasov *et al.* (SND Collaboration), Zh. Eksp. Teor. Fiz. **123**, 899 (2003) [J. Exp. Theor. Phys. **96**, 789 (2003)].
[6] R. R. Akhmetshin *et al.* (CMD-2 Collaboration), Phys. Lett. B **466**, 392 (1999).
[7] R. R. Akhmetshin *et al.* (CMD-2 Collaboration), Phys. Lett. B **562**, 173 (2003).
[8] F. Ambrosino *et al.* (KLOE Collaboration), Phys. Lett. B **669**, 223 (2008).
[9] D. Bisello *et al.* (DM2 Collaboration), *Nucl. Phys. Proc. Suppl.* 21, 111 (1991).
[10] M. N. Achasov *et al.*, Nucl. Instrum. Methods Phys. Res., Sect. A **598**, 31 (2009).

[11] V. M. Aulchenko *et al.*, Nucl. Instrum. Methods Phys. Res., Sect. A **598**, 102 (2009).
[12] A. Y. Barnyakov *et al.*, J. Instrum. **9**, C09023 (2014); Instrum. Exp. Tech. (USSR) **58**, 30 (2015).
[13] V. M. Aulchenko *et al.*, Nucl. Instrum. Methods Phys. Res., Sect. A **598**, 340 (2009).
[14] A. Romanov *et al.*, in *Proceedings of Particle Accelerator Conference PAC 2013, Pasadena, CA, USA, 2013* (JACoW, Geneva, 2013), p. 14, http://accelconf.web.cern.ch/AccelConf/pac2013/papers/proceed.pdf.
[15] M. N. Achasov *et al.* (SND Collaboration), Phys. Rev. D **88**, 054013 (2013).
[16] D. N. Shemyakin *et al.* (CMD-3 Collaboration), Phys. Lett. B **756**, 153 (2016).
[17] K. A. Olive *et al.* (Particle Data Group Collaboration), Chin. Phys. C **38**, 090001 (2014).
[18] E. A. Kuraev and V. S. Fadin, Yad. Fiz. **41**, 733 (1985) [Sov. J. Nucl. Phys. **41**, 466 (1985)].
[19] M. N. Achasov *et al.* (SND Collaboration), Phys. Rev. D **93**, 092001 (2016).
[20] R. Arnaldi *et al.* (NA60 Collaboration), Phys. Lett. B **757**, 437 (2016).
[21] K. W. Edwards *et al.* (CLEO Collaboration), Phys. Rev. D **61**, 072003 (2000).